Eur. Phys. J. D **23**, 443–447 (2003)
DOI: 10.1140/epjd/e2003-00073-1

THE EUROPEAN PHYSICAL JOURNAL D

Wavelength control in Er^{3+}-doped fluoride glasses laser by a coherent field

H.-F. Zhang[1,2,a], J.-H. Wu[1,2], and J.-Y. Gao[1,2,3]

[1] College of Physics, Jilin University, ChangChun 130023, P.R. China
[2] Key Lab. of Coherent Light, Atomic and Molecular Spectroscopy, Educational Ministry of China, P.R. China
[3] CCAST (World Laboratory), P.O. Box 8730, Beijing 100080, P.R. China

Received 9 October 2002
Published online 24 April 2003 –

Abstract. A five-level system to control the wavelength of the in-line amplifier by the quantum interference is proposed. It is found that the gains of the first and the second probe can be adjusted by changing the coherent field and the incoherent pumping. The new scheme may find its application in optical switch and optical communications.

PACS. 42.50.Gy Effects of atomic coherence on propagation, absorption, and amplification of light – 42.50.Hz Strong-field excitation of optical transitions in quantum systems; multi-photon processes; dynamic Stark shift

1 Introduction

Electromagnetically induced transparency (EIT) is one of the most studied directions of coherence and quantum interference, and most experimental and theoretical studies of quantum interference have so far focused on atomic gas media [1–3]. To understand quantum coherence and interference in crystals and for various potential device applications, EIT in solid media becomes more and more attractive [4,5]. Recent observation of EIT [6] in solid crystals [7] presents potential application of EIT for nonlinear optical processes, such as inversionless lasers [8], high-density optical memory [9], and enhanced four-wave mixing [10].

The incorporation of trivalent rare-earth ions in glass hosts has been known for many years as a technique to achieve efficient solid-state lasers and amplifiers [11]. For example, the praseodymium-doped fluoride fiber amplifier (PDFFA) has provided high gain and high output powers at wavelengths compatible with the second telecommunications window 1.3 μm [12]. The erbium-doped fluoride fiber amplifier, having a broad laser transition at 1.54 μm, is of specific interest in the field of optical communication [13]. In particular, an erbium doped fluorozirconate fibre amplifier has been fabricated which uses upconversion pumping at 0.801 μm to provide high gain at a wavelength of 0.85 μm [14]. In the future, all optical networks, whether based on optical time division multiplexing (OTDM) or wavelength division multiplexing (WDM), are likely to require the development of ultra-fast, data driven optical component, such as ultra-fast optical switches [15,16], wide-band optical amplifiers etc.

In this paper, a five-level scheme is proposed to change the wavelength of the in-line fiber amplifier and to adjust the gain of the in-line amplifier by controlling the Rabi frequency of a coherent field. Without the coherent field, the in-line amplifier, which is pumped by a semiconductor laser diode at 0.98 μm, emits at 1.54 μm. While when a coherent field is added, the in-line amplifier can emit at 0.81 μm, besides the gain at 1.54 μm. Under the action of strong coherent field, the gain at 1.54 μm disappears, and the gain at 0.81 μm becomes the dominant one. The idea of wavelength control proposed here may have its potential applications in optical switch and optical communications.

2 The model and equations

We consider a closed five-level system as shown in Figure 1. The energy-level scheme is relevant to the Er^{3+} ions in ZrF_4–BaF_2–LaF_3–AlF_3–NaF (ZBLAN) glass, where levels $|1\rangle$, $|2\rangle$, $|3\rangle$, $|4\rangle$ and $|5\rangle$ correspond to the energy levels of Er^{3+} ions $^4I_{15/2}$, $^4I_{13/2}$, $^4I_{11/2}$, $^4I_{9/2}$, and $^4S_{3/2}$, respectively. In this system, an incoherent pump process, interacting with the transition $|1\rangle \leftrightarrow |3\rangle$ and represented by a rate Λ, populates level $|2\rangle$ *via* fast phonon decay from level $|3\rangle$ to level $|2\rangle$. When the incoherent pumping is strong enough, population inversion can be established on the transition labeled $|2\rangle \leftrightarrow |1\rangle$, and then the probe on $|2\rangle \leftrightarrow |1\rangle$ can be amplified. A coherent driving field E_c with Rabi frequency Ω_c interacts with the transition

[a] e-mail: qol@mail.jlu.edu.cn

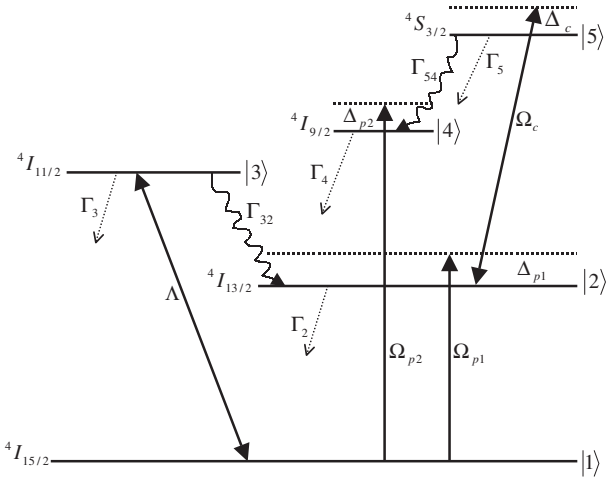

Fig. 1. Schematic diagram of a five-level system where levels $|1\rangle$, $|2\rangle$, $|3\rangle$, $|4\rangle$ and $|5\rangle$ are corresponding to energy levels of Er^{3+} ions in ZBLAN glass $^4I_{15/2}$, $^4I_{13/2}$, $^4I_{11/2}$, $^4I_{9/2}$ and $^4S_{3/2}$, respectively.

$|2\rangle \leftrightarrow |5\rangle$, and populates level $|4\rangle$ *via* fast phonon decay from level $|5\rangle$ to level $|4\rangle$. The role of the coherent driving field E_c is not only to populate level $|4\rangle$, but also split level $|2\rangle$ into two dressed sublevels. Thus, the population inversion and the probe amplification on the transition labeled $|4\rangle \leftrightarrow |1\rangle$ could be controlled by the coherent field. The first probe field E_{p1} with Rabi frequency Ω_{p1} interacts with the transition labeled $|1\rangle \leftrightarrow |2\rangle$, while the second probe field E_{p2} with Rabi frequency Ω_{p2} interacts with the transition labeled $|1\rangle \leftrightarrow |4\rangle$. $\Gamma_5 = \Gamma_{51} + \Gamma_{52} + \Gamma_{53} + \Gamma_{54}$ is the spontaneous decay rate of level $|5\rangle$, $\Gamma_4 = \Gamma_{41}+\Gamma_{42}+\Gamma_{43}$ is the spontaneous decay rate of level $|4\rangle$, $\Gamma_3 = \Gamma_{31} + \Gamma_{32}$ is the spontaneous decay rate of level $|3\rangle$, and $\Gamma_2 = \Gamma_{21}$ is the spontaneous decay rate of level $|2\rangle$.

Using the standard semiclassical methods [17], under the dipole approximation and the rotating wave approximation, the interaction Hamiltonian H_I can be represented in the interaction picture by:

$$H_I = -\Delta_{p1}|2\rangle\langle 2| - \Delta_{p2}|4\rangle\langle 4| - (\Delta_{p1}+\Delta_c)|5\rangle\langle 5| - (\Omega_{p1}|2\rangle\langle 1| + \Omega_{p2}|4\rangle\langle 1| + \Omega_c|5\rangle\langle 2| + \text{c.c}) \quad (1)$$

where the detunings of the probes and the coherent field are defined as: $\Delta_{p1} = \omega_{p1} - (\omega_2 - \omega_1)$, $\Delta_{p2} = \omega_{p2} - (\omega_4 - \omega_1)$, $\Delta_c = \omega_c - (\omega_5 - \omega_2)$, respectively; the Rabi frequencies Ω_c, Ω_{p1} and Ω_{p2} are defined as: $\Omega_c = \mu_{52}E_c/2\hbar$, $\Omega_{p1} = \mu_{21}E_{p1}/2\hbar$, $\Omega_{p2} = \mu_{41}E_{p2}/2\hbar$, respectively. Just for simplicity in calculation, Ω_c, Ω_{p1} and Ω_{p2} are always chosen to be real in this paper.

Assuming $\hbar = 1$ for simplicity, the master equation of motion for the density operator in an arbitrary multi-level atomic system in the interaction picture can be written as:

$$\frac{\partial\rho}{\partial t} = -i[H_I, \rho] + \Lambda\rho. \quad (2)$$

By expanding equation (2), we can easily arrive at their equations of motion:

$$\begin{aligned}
\dot\rho_{11} &= \Lambda(\rho_{33}-\rho_{11}) + \Gamma_{21}\rho_{22} + \Gamma_{31}\rho_{33} + \Gamma_{41}\rho_{44} + \Gamma_{51}\rho_{55} \\
&\quad + i\Omega_{p1}^*\rho_{21} - i\Omega_{p1}\rho_{12} + i\Omega_{p2}^*\rho_{41} - i\Omega_{p2}\rho_{14} \\
\dot\rho_{22} &= -\Gamma_{21}\rho_{22} + \Gamma_{32}\rho_{33} + \Gamma_{42}\rho_{44} + \Gamma_{52}\rho_{55} \\
&\quad + i\Omega_{p1}\rho_{12} - i\Omega_{p1}^*\rho_{21} + i\Omega_c^*\rho_{52} - i\Omega_c\rho_{25} \\
\dot\rho_{33} &= -\Lambda(\rho_{33}-\rho_{11}) - \Gamma_{31}\rho_{33} - \Gamma_{32}\rho_{33} + \Gamma_{43}\rho_{44} + \Gamma_{53}\rho_{55} \\
\dot\rho_{44} &= -\Gamma_{41}\rho_{44} - \Gamma_{42}\rho_{44} - \Gamma_{43}\rho_{44} + \Gamma_{54}\rho_{55} \\
&\quad + i\Omega_{p2}\rho_{14} - i\Omega_{p2}^*\rho_{41} \\
\dot\rho_{21} &= -(\gamma_{21} - i\Delta_{p1})\rho_{21} + i\Omega_{p1}(\rho_{11}-\rho_{22}) \\
&\quad + i\Omega_c\rho_{51} - i\Omega_{p2}\rho_{24} \\
\dot\rho_{31} &= -\gamma_{31}\rho_{31} - i\Omega_{p1}\rho_{32} - i\Omega_{p2}\rho_{34} \\
\dot\rho_{41} &= -(\gamma_{41} - i\Delta_{p2})\rho_{41} + i\Omega_{p2}(\rho_{11}-\rho_{44}) - i\Omega_{p1}\rho_{42} \\
\dot\rho_{51} &= -(\gamma_{51} - i(\Delta_{p1}+\Delta_c))\rho_{51} \\
&\quad + i\Omega_c\rho_{21} - i\Omega_{p1}\rho_{52} - i\Omega_{p2}\rho_{54} \\
\dot\rho_{32} &= -(\gamma_{32} + i\Delta_{p1})\rho_{32} - i\Omega_{p1}\rho_{31} - i\Omega_c\rho_{35} \\
\dot\rho_{42} &= -(\gamma_{42} - i\Delta_{p2} + i\Delta_{p1})\rho_{42} \\
&\quad + i\Omega_{p2}\rho_{12} - i\Omega_{p1}\rho_{41} - i\Omega_c\rho_{45} \\
\dot\rho_{52} &= -(\gamma_{52} - i\Delta_c)\rho_{52} + i\Omega_c(\rho_{22}-\rho_{55}) - i\Omega_{p1}\rho_{51} \\
\dot\rho_{43} &= -(\gamma_{43} - i\Delta_{p2})\rho_{43} + i\Omega_{p2}\rho_{13} \\
\dot\rho_{53} &= -(\gamma_{53} - i(\Delta_{p1}+\Delta_c))\rho_{53} + i\Omega_c\rho_{23} \\
\dot\rho_{54} &= -(\gamma_{54} - i(\Delta_c + \Delta_{p1} - \Delta_{p2}))\rho_{54} + i\Omega_c\rho_{24} - i\Omega_{p2}^*\rho_{51} \\
&\rho_{11}+\rho_{22}+\rho_{33}+\rho_{44}+\rho_{55} = 1 \\
&\rho_{ij} = \rho_{ji}^* \qquad (3)
\end{aligned}$$

where Γ_{ij} designates the population spontaneous damping from $|i\rangle$ to $|j\rangle$, while γ_{ij} refers to the coherence decay rate between $|i\rangle$ and $|j\rangle$. In the radiative limit, the coherence decay rates are given by:

$$\begin{aligned}
\gamma_{54} &= (\Gamma_{51}+\Gamma_{52}+\Gamma_{53}+\Gamma_{54}+\Gamma_{41}+\Gamma_{42}+\Gamma_{43})/2 \\
\gamma_{53} &= (\Gamma_{51}+\Gamma_{52}+\Gamma_{53}+\Gamma_{54}+\Gamma_{31}+\Gamma_{32}+\Lambda)/2 \\
\gamma_{52} &= (\Gamma_{51}+\Gamma_{52}+\Gamma_{53}+\Gamma_{54}+\Gamma_{21})/2 \\
\gamma_{51} &= (\Gamma_{51}+\Gamma_{52}+\Gamma_{53}+\Gamma_{54}+\Lambda)/2 \\
\gamma_{43} &= (\Gamma_{41}+\Gamma_{42}+\Gamma_{43}+\Gamma_{31}+\Gamma_{32}+\Lambda)/2 \\
\gamma_{42} &= (\Gamma_{41}+\Gamma_{42}+\Gamma_{43}+\Gamma_{21})/2 \\
\gamma_{41} &= (\Gamma_{41}+\Gamma_{42}+\Gamma_{43}+\Lambda)/2 \\
\gamma_{32} &= (\Gamma_{31}+\Gamma_{32}+\Gamma_{21}+\Lambda)/2 \\
\gamma_{31} &= (\Gamma_{31}+\Gamma_{32}+\Lambda+\Lambda)/2 \\
\gamma_{21} &= (\Gamma_{21}+\Lambda)/2. \qquad (4)
\end{aligned}$$

The steady state solutions of the set of equation (3) can be obtained by setting the time derivatives to zero. They are very complicated since they depend on many parameters, such as Λ, Ω_c, Ω_{p1}, Ω_{p2}, Δ_c, Δ_{p1}, Δ_{p2}, Γ_{ij}, γ_{ij}. To find the optimal results and the corresponding conditions, we have to resort to the numerical calculation in next section.

In the limit of a weak probe, the gain-absorption coefficient on transition $|2\rangle \leftrightarrow |1\rangle$ ($|4\rangle \leftrightarrow |1\rangle$) is proportional to the imaginary part of ρ_{12} (ρ_{14}), and we obtain the probe gain if $\text{Im}(\rho_{12}) > 0$ ($\text{Im}(\rho_{14}) > 0$).

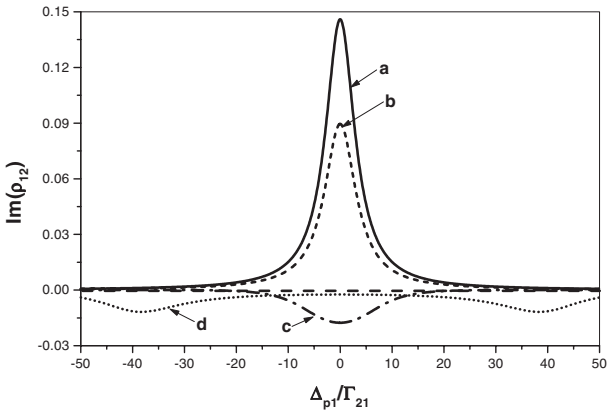

Fig. 2. Plots of the dimensionless first probe gain coefficient $\mathrm{Im}(\rho_{12})$ *versus* the first probe detuning $\Delta_{\mathrm{p1}}/\Gamma_{21}$ for different Rabi frequencies of the resonant coherent field. The curves a, b, c, d correspond to $\Omega_{\mathrm{c}} = 0.0$, 2.0, 8.0, 40.0, respectively. The other parameters used are $\Gamma_{31} = 1.0$, $\Gamma_{32} = 20.0$, $\Gamma_{41} = 1.0$, $\Gamma_{42} = 0.3$, $\Gamma_{43} = 0.0$, $\Gamma_{51} = 8.0$, $\Gamma_{52} = 3.0$, $\Gamma_{53} = 0.3$, $\Gamma_{54} = 15.0$, $\Omega_{\mathrm{p1}} = 1.0$, $\Omega_{\mathrm{p2}} = 0.0$, $\Delta_{\mathrm{p2}} = 0.0$, the incoherent pumping rate $\Lambda = 5.0$.

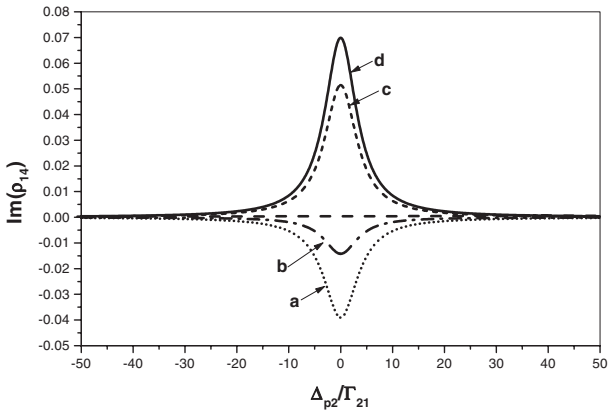

Fig. 3. Plots of the dimensionless second probe gain coefficient $\mathrm{Im}(\rho_{14})$ *versus* the second probe detuning $\Delta_{\mathrm{p2}}/\Gamma_{21}$ for different Rabi frequencies of the resonant coherent field. The curves a, b, c, d correspond to $\Omega_{\mathrm{c}} = 0.0$, 2.0, 8.0, 40.0, respectively. The other parameters used are same as those in Figure 2 except $\Omega_{\mathrm{p1}} = 0.0$, $\Omega_{\mathrm{p2}} = 1.0$, $\Delta_{\mathrm{p1}} = 0.0$. The incoherent pumping rate $\Lambda = 5.0$.

3 Results and discussion

There are two important factors, the incoherent pump and the coherent field, which can affect the light amplification of the two probes remarkably. The incoherent pumping enhances the gain of the first probe, but the coherent field weakens it by pumping ionic atoms from level $|2\rangle$ to level $|5\rangle$. However, both the incoherent pumping and the coherent field enhance the gain of the second probe.

In the following, we discuss the effects of the incoherent pumping and the coherent field on the gain of the two probes by numerical solutions, and give a few important conclusions on wavelength control of the in-line amplifier.

Based on references [18,19], it is reasonable that we always chose the parameters as: $\Gamma_{31} = 1.0$, $\Gamma_{32} = 20.0$, $\Gamma_{41} = 1.0$, $\Gamma_{42} = 0.3$, $\Gamma_{43} = 0.0$, $\Gamma_{51} = 8.0$, $\Gamma_{52} = 3.0$, $\Gamma_{53} = 0.3$, $\Gamma_{54} = 15.0$. In this paper, all other parameters are scaled by Γ_{21}.

To comprehend the effect of atomic coherence on wavelength control of the in-line amplifier, we depict the variation of gains of the two probes *vs.* corresponding probe detunings in Figures 2 and 3 when the incoherent pumping and the coherent field are in action and not in action. It is well-known that, without the coherent field Ω_{c} and the second probe Ω_{p2}, the five-level system can be considered as a three-level system composed of $|1\rangle$, $|2\rangle$, and $|3\rangle$, and emits at 1.54 μm (see curve a in Fig. 2) when it is pumped by a semiconductor laser diode at 0.98 μm. In the presence of the resonant coherent field on transition $|2\rangle \leftrightarrow |5\rangle$, the gain decreases because the coherent field splits level $|2\rangle$ into two dressed sublevels, and at the same time, part of the population is pumped to higher level $|5\rangle$, as shown by curve b in Figure 2. The stronger the Rabi frequency of the coherent field becomes, the more the gain of the first probe field reduces. The gain may changes into absorption when the coherent field becomes large, as shown by curve c in Figure 2. The gain (absorption) at $\Delta_{\mathrm{p1}} = 0.0$ reaches zero when the Rabi frequency of the coherent field is very strong, $\Omega_{\mathrm{c}} = 40.0$, as shown by curve d in Figure 2. Note that with the increasing of Rabi frequency Ω_{c}, population inversion on transition $|1\rangle \leftrightarrow |2\rangle$ is decreasing (we checked, but have not shown the graphic results here). When the first probe goes from amplification to transparency, the second probe changes from absorption to amplification. Without the coherent field Ω_{c} and the first probe field Ω_{p1}, the second probe displays absorption, as shown by curve a in Figure 3. When $\Omega_{\mathrm{c}} = 2.0$, the absorption of the second probe decreases, as shown by curve b in Figure 3. When $\Omega_{\mathrm{c}} = 8.0$, the second probe has been amplified, and a new laser wavelength appears at 0.81 μm, as shown by curve c in Figure 3, and it becomes much larger when $\Omega_{\mathrm{c}} = 40.0$, as shown by curve d in Figure 3. In this condition, the population inversion has been established between levels $|4\rangle$ and $|1\rangle$.

There are three parameters which influence the gain of the two probes, *i.e.*, the incoherent pumping rate Λ, the Rabi frequency of the coherent field Ω_{c} and its detuning Δ_{c}. To show the effect of the incoherent pumping rate Λ on the probe, we depict the gain (absorption) amplitudes of the first probe, $\mathrm{Im}(\rho_{12})$, at $\Delta_{\mathrm{p1}} = 0.0$ and the second probe, $\mathrm{Im}(\rho_{14})$, at $\Delta_{\mathrm{p2}} = 0.0$ when the Rabi frequency of the resonant coherent field is $\Omega_{\mathrm{c}} = 0.0$ and $\Omega_{\mathrm{c}} = 10.0$ in Figures 4a and 4b, respectively. In the case of $\Omega_{\mathrm{c}} = 0.0$, the first probe gain $\mathrm{Im}(\rho_{12})$ does not occur before the population inversion between level $|2\rangle$ and level $|1\rangle$ is established at $\Lambda/\Gamma_{21} = 1.11$. After this point, the first probe gain appears, and then it becomes larger and larger with the increasing of Λ before it reaches a saturation, as shown by curve $\mathrm{Im}(\rho_{12})$ in Figure 4a. At the meantime, the absorption of the second probe decreases with the increasing of the incoherent pump rate Λ, but the second probe gain $\mathrm{Im}(\rho_{14})$ never appears because there is no way for the establishment of population inversion

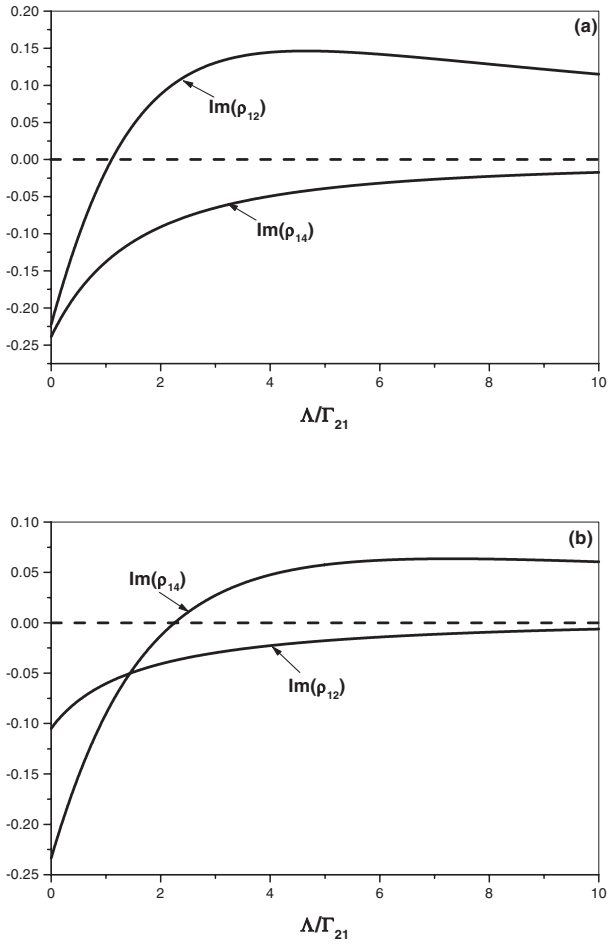

Fig. 4. (a) Plots of the dimensionless probe gain coefficients $\mathrm{Im}(\rho_{12})$ at $\Delta_{\mathrm{p1}} = 0.0$ and $\mathrm{Im}(\rho_{14})$ at $\Delta_{\mathrm{p2}} = 0.0$ *versus* the incoherent pumping Λ/Γ_{21} at different Rabi frequencies of the resonant coherent field. (a) $\Omega_{\mathrm{c}} = 0.0$. (b) $\Omega_{\mathrm{c}} = 10.0$. The other parameters used are same as those in Figure 2 except $\Omega_{\mathrm{p1}} = 1.0$, $\Omega_{\mathrm{p2}} = 1.0$.

between level $|4\rangle$ and level $|1\rangle$, as shown by curve $\mathrm{Im}(\rho_{14})$ in Figure 4a. In the case of $\Omega_{\mathrm{c}} = 10.0$, the situation is completely different. The first probe gain $\mathrm{Im}(\rho_{12})$ changes into absorption, and the absorption decreases with the increasing of the incoherent pumping rate Λ, as shown by curve $\mathrm{Im}(\rho_{12})$ in Figure 4b, while the absorption of the second probe $\mathrm{Im}(\rho_{14})$ changes into amplification, and it increases with the increasing of the incoherent pump rate Λ, this is because strong incoherent pump and strong coherent field pump more and more population into level $|4\rangle$.

In Figure 5, we depict the gain (absorption) amplitudes of the first probe $\mathrm{Im}(\rho_{12})$ at $\Delta_{\mathrm{p1}} = 0.0$, and the second probe $\mathrm{Im}(\rho_{14})$ at $\Delta_{\mathrm{p2}} = 0.0$ *vs.* the Rabi frequency of the resonant coherent field Ω_{c} when the incoherent pump rate is fixed at $\Lambda = 5.0$, respectively. The first probe amplification can be observed when the Rabi frequency of the coherent field Ω_{c} is small, but it decreases very fast at the beginning with the increasing of the Rabi frequency of the coherent field Ω_{c}, then changes into absorption, and approaches to zero at last, the electromagnetically induced

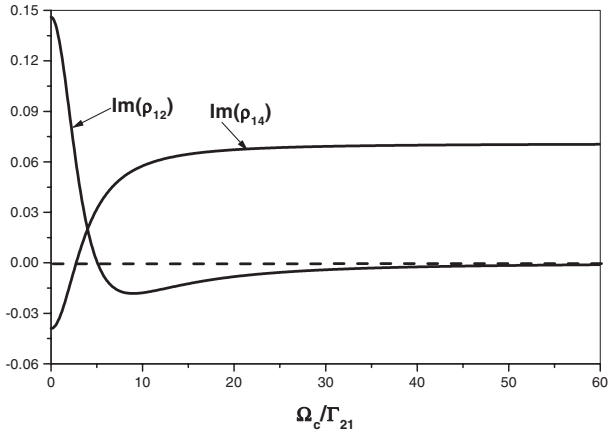

Fig. 5. Plots of the dimensionless probe gain coefficients $\mathrm{Im}(\rho_{12})$ at $\Delta_{\mathrm{p1}} = 0.0$ and $\mathrm{Im}(\rho_{14})$ at $\Delta_{\mathrm{p2}} = 0.0$ *versus* the Rabi frequency of the resonant coherent field $\Omega_{\mathrm{c}}/\Gamma_{21}$ at the incoherent pumping $\Lambda = 5.0$. The other parameters used are same as those in Figure 2 except $\Omega_{\mathrm{p1}} = 1.0$, $\Omega_{\mathrm{p2}} = 1.0$.

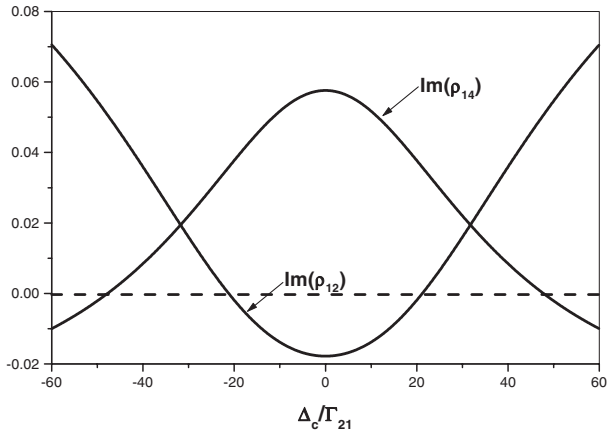

Fig. 6. Plots of the dimensionless probe gain coefficients $\mathrm{Im}(\rho_{12})$ at $\Delta_{\mathrm{p1}} = 0.0$ and $\mathrm{Im}(\rho_{14})$ at $\Delta_{\mathrm{p2}} = 0.0$ *versus* the detuning of the coherent field $\Delta_{\mathrm{c}}/\Gamma_{21}$ at the incoherent pumping $\Lambda = 5.0$, and the Rabi frequency of the coherent field $\Omega_{\mathrm{c}} = 10.0$. The other parameters used are same as those in Figure 2 except $\Omega_{\mathrm{p1}} = 1.0$, $\Omega_{\mathrm{p2}} = 1.0$.

transparency was observed. However, the second probe goes a different direction. It changes from negative to positive quickly, then approaches a saturating value when Ω_{c} exceeds a certain value. So the incoherent pumping and the coherent field are essential for amplification of the second probe.

In Figure 6, we depict the gain (absorption) amplitudes of the first probe $\mathrm{Im}(\rho_{12})$ at $\Delta_{\mathrm{p1}} = 0.0$, and the second probe $\mathrm{Im}(\rho_{14})$ at $\Delta_{\mathrm{p2}} = 0.0$ *vs.* the detuning of the coherent field Δ_{c} when the incoherent pump rate $\Lambda = 5.0$, and the Rabi frequency of the coherent field $\Omega_{\mathrm{c}} = 10.0$. It is found that the gains of the two probes $\mathrm{Im}(\rho_{12})$ and $\mathrm{Im}(\rho_{14})$ are both symmetrical about the zero detuning of the coherent field. The gains for the first probe and the second probe reaches their minimum and maximum at the zero detuning, then change to different directions when the detuning becomes large. This is easily to be

understood because the large detuning means weak action of the coherent field.

4 Conclusions

In this paper, a five-level model is proposed where the gains of two probes can be modified by a coherent field. Effects of the incoherent pump and the coherent field on the gains of two probes are studied, namely, the gain of the first probe can go from amplification to absorption, and at the same time, the amplification of the second probe field can be changed from negative to positive under the action of the coherent field. The system developed here may find its application in optical switch and optical communications.

The authors would like to thank the support from the National Natural Science Foundation of China, the support from the Doctoral Program Foundation of Institution of Higher Education of China, and the support from the Educational Ministry of China.

References

1. Y. Zhu, M. Xiao, Y. Zhao, Phys. Rev. A **49**, 4016 (1994)
2. S.E. Harris, J.E. Field, A. Imamoglu, Phys. Rev. Lett. **64**, 1107 (1990)
3. K.J. Boller, A. Imamoglu, S.E. Harris. Phys. Rev. Lett. **66**, 2593 (1991)
4. B.S. Ham, P.R. Hemmer, M.S. Shahriar, Opt. Commun. **144**, 227 (1997)
5. M. Artoni, G.C. La Rocca, F. Bassani, Europhys. Lett. **49**, 445 (2000)
6. S.E. Harris, Phys. Today **50**(7), 36 (1997)
7. Y. Zhao, C. Wu, B.S. Ham, M.S. Shahriar, P.R. Hemmer, Opt. Commun. **144**, 227 (1997)
8. A.S. Zibrov, M.D. Lukin, D.E. Nikonov, L. Hollberg, M.O. Scully, V.L. Velichansky, H.G. Robinson, Phys. Rev. Lett. **75**, 1499 (1995)
9. B.S. Ham, M.S. Shahriar, M.K. Kim, P.R. Hemmer, Opt. Lett. **22**, 1849 (1997)
10. B.S. Ham, M.S. Shahriar, Opt. Lett. **24**, 86 (1999)
11. C.F. Rapp, "laser glasses", in *Handbook of Laser Science and Technology*, edited by M.J. Weber (CRC Press, West Palm Beach, FL, 1987), Vol. V, Part III
12. T.J. Whitley, J. Lightw. Technol. **13**, 744 (1995)
13. *Proc. of 17th European Conference on Optical Communication ECOC'91*, Paris, 9-12 Sept. 1991, paper WeC9-6, pp. 601-604
14. T.J. Whitley *et al.*, Electron. Lett. **27**, 184 (1991)
15. S.L. Danielsen *et al.*, Electron. Lett. **32**, 1686 (1996)
16. X.-M. Su, J.-Y. Gao, Phys. Lett. A **264**, 346 (2000)
17. M. Sargent III, M.O. Scully, W.E. Lamb Jr, *Laser Physics* (Addison-Wesley, Reading, MA, 1974)
18. M.D. Shinn, W.A. Sibley, Phys. Rev. B **27**, 6635 (1983)
19. E. Snitzer, R. Woodcock, Appl. Phys. Lett. **6**, 45 (1965)